AMSI VACATION RESEARCH SCHOLARSHIPS 2019–20

EXPLORE THE MATHEMATICAL SCIENCES THIS SUMMER

Modelling of Tissue Formation on 3D-printed Scaffolds

Reuben Hill

Supervised by Dr Pascal Buenzli &

Prof. Matthew Simpson

Queensland University of Technology

Vacation Research Scholarships are funded jointly by the Department of Education and Training and the Australian Mathematical Sciences Institute.

AMSI AUSTRALIAN MATHEMATICAL SCIENCES INSTITUTE

Australian Government Department of Education

Abstract

The advent of 3D-printing has provided important opportunities for Medical Science, particularly the field of Tissue Engineering, where sufficient advances in the technology could lead to widespread production of artificially printed organs or skin. In this project, we developed a finite difference method (FDM) based model which can solve reaction-diffusion partial differential equations (PDEs) in 1-2 dimensions to simulate the proliferation of cells across an empty, square-framed lattice on a microscopic scale. Furthermore, we recorded the time taken for simulated cells to proliferate to capacity (time to 'bridge') across a range of systems with varying domain size and general diffusivity. We additionally investigated the use of Likelihood Profiling methods to generate intervals of probable parameter values in example exercises, given observational data. In future, we aim to apply these Likelihood Profiling methods to the PDE systems also investigated in this work.

1 Introduction

Tissue engineering aims to use experimental methodologies to replace the need for human tissue and organ donation by artificially growing new tissues and organs for transplantation. Mathematical modelling will play a key role in interpreting, quantifying and ultimately optimising experimental protocols in this field. This project will illustrate how mathematical models can be used to provide new insight into experimental observations in the field of tissue engineering. The results for this project were two-fold: firstly, we developed a discrete computational model of cell migration and proliferation, where these rates are coupled to the availability of extracellular matrix [2]. Using approximate conservation arguments, we derived a mean-field partial differential equation description in terms of cell density $n(x, y, t)$. Secondly, we numerically determined intervals of probable parameter values for example models, given synthetically generated observational data, using a Bayesian framework [3], with the intent of applying the same methodology to the aforementioned PDE model in future work.

Statement of Authorship

- Dr Pascal Buenzli and Professor Matthew Simpson came up with the idea for the research project, provided previous research and experimental results for analysis, as well as write the introduction and proofread this document.
- Reuben Hill developed the MATLAB code to perform the project tasks, as well as write this report.

2 Methods

2.1 Partial Differential Equations

This investigation aims to use numerical methods to simulate the proliferation of cells in a monolayer over time, modelled with the generalised Porous-Fisher equation:

$$\frac{\partial n}{\partial t} = D\nabla \cdot \left[\left(\frac{n}{K}\right)^p \nabla n\right] + \lambda n\left[1 - \frac{n}{K}\right] \tag{1}$$

Where n denotes the density of cells at a given point in spacetime, measured in cells/μm^2. D is cell diffusivity, μm^2/day. K is cell carrying capacity, p is a dimensionless constant and λ is proliferation rate, 1/day. For the purposes of testing and verification, several 'sub-systems' based off the Porous-Fisher equation were simulated using numerical methods in MATLAB. These problems were solved in a one-dimensional domain, using system parameters and initial/boundary conditions as summarised below.

2.1.1 Outward Diffusion Systems

By setting $\lambda = 0 = p$ in (1) we retrieve the heat equation, which was used as the initial test scenario to solve (see (2)). The second scenario took a slightly more complicated diffusion process, setting $\lambda = 0, p = 1$, resulting in (3). Unless otherwise specified, the chosen parameter values for 1D systems were: $D = 2400$, $K = n_0 = 2 \times 10^{-3}$.

$$\frac{\partial n}{\partial t} = D\frac{\partial^2 n}{\partial x^2} \tag{2}$$

$$\frac{\partial n}{\partial t} = D\frac{\partial}{\partial x}\left[\left(\frac{n}{K}\right)^p \frac{\partial n}{\partial x}\right] \tag{3}$$

Both systems had the same initial and boundary conditions enforced:

$$n(x, t=0) = \delta(x) = \begin{cases} 1 & x = 0 \\ 0 & x \neq 0 \end{cases}$$

$$n(x = \frac{-L}{2}, t) = n(x = \frac{L}{2}, t) = 0$$

$$|x| \leq \frac{L}{2},\ t \geq 0$$

Under these conditions, both of these systems possess analytical solutions, unlike the generalised Porous-Fisher model. On an infinite domain, with an initial condition given by the dirac-delta function, $\delta(x)$, Walker [1] provides the following solutions :

Heat Equation:

$$n(x,t) = \frac{Q}{2\sqrt{\pi D t}} \exp\left(\frac{-x^2}{4Dt}\right) \tag{4}$$

Where Q is the density of cells present at the initial condition.

Complex Diffusion Equation:

$$n(x,t) = \begin{cases} \frac{K}{\lambda(t)}\left[1 - \left(\frac{x}{r_0\lambda(t)}\right)^2\right]^{1/p} & |x| \leq r_0\lambda(t) \\ 0 & |x| > r_0\lambda(t) \end{cases} \tag{5}$$

$$\text{Where } \lambda(t) = \left(\frac{t}{t_0}\right)^{\frac{1}{2+p}}$$

$$r_0 = \frac{Q\Gamma(\frac{1}{p} + 1.5)}{\sqrt{\pi}K\Gamma(\frac{1}{p} + 1)}$$

$$t_0 = \frac{r_0^2 p}{2D(p+2)}$$

These analytical solutions were used to verify the accuracy of the FDM-solver's numerical solutions when testing the one-dimensional problems.

2.1.2 Travelling Wave Diffusion System

To analyse the behaviour of cell diffusion/proliferation system with a source term, we took (1) and set $p = 0, K = 1$ to retrieve:

$$\frac{\partial n}{\partial t} = D\frac{\partial^2 n}{\partial x^2} + \lambda n(1-n) \tag{6}$$

The system's initial and boundary conditions were set as:

$$0 \leq x \leq L,\ t \geq 0$$

$$n(x, t=0) = \delta(x) = \begin{cases} 1 & x = 0 \\ 0 & x \neq 0 \end{cases}$$

$$(x = 0, t) = n\,(x = L, t) = 0$$

Under these conditions, the profile of the solution over time is a travelling wave (with no 'proper' analytical solution), which can be approximated numerically. Walker [1], showed the steady-state velocity of the travelling wave has the upper bound:

$$c = 2\sqrt{\lambda D} \tag{7}$$

The primary metric for determining the accuracy of numerical approximations is equation (7), as well as *a priori* knowledge of the expected system behaviour from Walker [1].

2.1.3 2D Porous-Fisher Simulations

After simulating the one-dimensional sub-systems and verifying their accuracy, we progressed to solving Porous-Fisher in two dimensions with realistic parameter values provided from previous research [4]. These simulations solve equation (1) with the following system conditions:

$$\left.\frac{\partial n}{\partial x}\right|_{\partial V} \cdot \hat{m} = \left.\frac{\partial n}{\partial y}\right|_{\partial V} \cdot \hat{m} = 0$$

$$n(x, y, t=0) = \begin{cases} n_0, & x = 0 \text{ or } x = L \\ n_0, & y = 0 \text{ or } y = L \\ 0, & \text{Otherwise} \end{cases}$$

$$0 \leq x, y \leq L,\ t \geq 0$$

Where $\hat{m}$ are unit-normals oriented outward from the system boundaries, ∂V.

Parameter	Value
p	1
K	2×10^{-3}
λ	0.48
D	2400
n_0	2×10^{-3}

2.2 FDM Model

To solve Porous-Fisher numerically, the Finite Difference Method (FDM) was used to discretise the working domains into an $I \times J$ node mesh, with uniform spacing across both dimensions:

$$\frac{\partial n_{ij}}{\partial t} \coloneqq \frac{\partial}{\partial t} n(x = (i-1)h_x, y = (j-1)h_y, t) \tag{8}$$

$$1 \leq i \leq I,\ 1 \leq j \leq J,\ i, j \in \mathbb{N}$$

Where h is the spacing between nodes, $h_x = \frac{L_x}{I-1}$, $h_y = \frac{L_y}{J-1}$ and L is the domain length in the relevant direction.

First-order forward differencing was used to generate the system of resultant equations during the discretisation process. In the differencing process, values for the function $D(n) = (\frac{n}{K})^p$ were averaged between nodes. Following the spatial discretisations, the Runge-Kutta method was implemented to solve the remaining system of ordinary differential equations (ODEs), using MATLAB's ode45 function. Square grids were used for the full, two-dimensional simulations of Porous-Fisher ($I \times I$), over boundaries of varying lengths, L. For the one-dimensional sub-systems, rectangular grids were used to calculate results, generally $3 \times J$, with no-flux vertical boundary conditions enforced: results shown in this paper are extracted from the central row.

2.2.1 Time to Bridge

Another objective of the FDM-solver alongside simulating cell-proliferation was to measure the 'Time to Bridge', T_b, which is the time taken for the system to reach capacity by 'filling' the scaffold. Within the FDM-solver, we defined any node with a cell density greater than half of the carrying capacity to be considered 'bridged', and took T_b as the time taken to

bridge the central-most node (recall the initial condition). It is worth noting that the systems investigated this way used a different proliferation rate to the 2D simulations, here we chose $\lambda = 24\ln(2)/15$.

2.3 Likelihood Profiling

An additional objective of this project was to develop MATLAB software to perform likelihood profiling to generate intervals of probable parameter values to fit model equations to observed data. In the context of this work, these techniques were only applied to example problems, with the aim to perform likelihood profiling on the FDM-solver's parameters in future work.

The example problems examined used multiple-parameter models, where each parameter was individually profiled. Likelihood profiling utilises the Bayesian concept of the *likelihood function*, $\mathcal{L}(\boldsymbol{\theta}; \boldsymbol{y})$, which is a measure of goodness-of-fit for an n-tuple combination of parameters given the observed data. We can filter out 'nuisance parameters' in order to profile a single variable of interest.

Likelihood Function:

$$\mathcal{L}(\boldsymbol{\theta}; \boldsymbol{y}) = \frac{\prod_{i=1}^{n} p(y_i|\boldsymbol{\theta})}{\sup_{\theta} \prod_{i=1}^{n} p(y_i|\boldsymbol{\theta})} \tag{9}$$

Where $p(y_i|\boldsymbol{\theta})$ is the probability density function (PDF) of an observation's occurrence, given the parameter values. Say $\boldsymbol{\theta}$ is comprised of a variable of interest, α and 'nuisance variables', β, which are not. We can then optimise-out the nuisance variables to profile only α:

$$\mathcal{L}(\alpha; \boldsymbol{y}, \boldsymbol{\beta}) = \frac{\sup_{\beta} \prod_{i=1}^{n} p(y_i|\alpha, \boldsymbol{\beta})}{\sup_{\alpha,\beta} \prod_{i=1}^{n} p(y_i|\alpha, \boldsymbol{\beta})} \tag{10}$$

The values of the likelihood profile over an interval can be numerically calculated, using MATLAB's fminsearch functionality to determine optimising values of $\alpha, \boldsymbol{\beta}$.

In order to perform likelihood profiling, several underlying assumptions must be met for results to be informative. Firstly, in order to obtain meaningful results we must assume that the observed data, $\boldsymbol{y^o}$ is equal to predicted results from a model, plus some normally distributed

error, ϵ. From this, it follows that the observed data is normally distributed, where the mean is determined by the predicted value from the model and there is some variance.

$$\boldsymbol{y^o} = \boldsymbol{y(x|\theta)} + \boldsymbol{\epsilon}$$
$$y_i^o \sim N(y(x_i|\boldsymbol{\theta}), \sigma^2)$$

With these assumptions, we now have a closed form PDF for the observed data from which to calculate the likelihood.

2.3.1 Quadratic Example Problem

The initial example analysed using Likelihood Profiling took observations synthetically generated by taking a quadratic equation and adding Gaussian noise:

$$y(x|a,b) = ax + bx^2 \tag{11}$$

For this example, the true values $(a,b) = (1,3)$. Forty observations were taken between $0 \leq x \leq 1$ from (11), with randomly generated noise added. This exercise was repeated with differing levels of variance, further discussed in Results.

2.3.2 ODE Example Problem

A more complicated, ODE problem was also profiled, where the model equation was the solution to:

$$\frac{dy}{dt} = ay + b \tag{12}$$

With initial condition $y(0) = 3$ and true values $(a,b) = (1,2)$. Like the previous example, 40 observations were drawn over $0 \leq t \leq 1$ with equation (12).

3 Results

3.1 FDM-Solver

3.1.1 Outward Diffusion

Due to the exponential nature of equation (4) requiring an infinite domain to be completely valid, it follows that the numerical results can only be viewed as accurate for sufficiently large

domain sizes. However, with respect to the complex diffusion system, the analytical solution provided is fully correct for finite domains.

Several simulations for each system were performed, using the parameters outlined in Methods, over varying domain lengths (100, 300, 1000 μm), for which the numerical results of each profile were compared to the analytical solution.

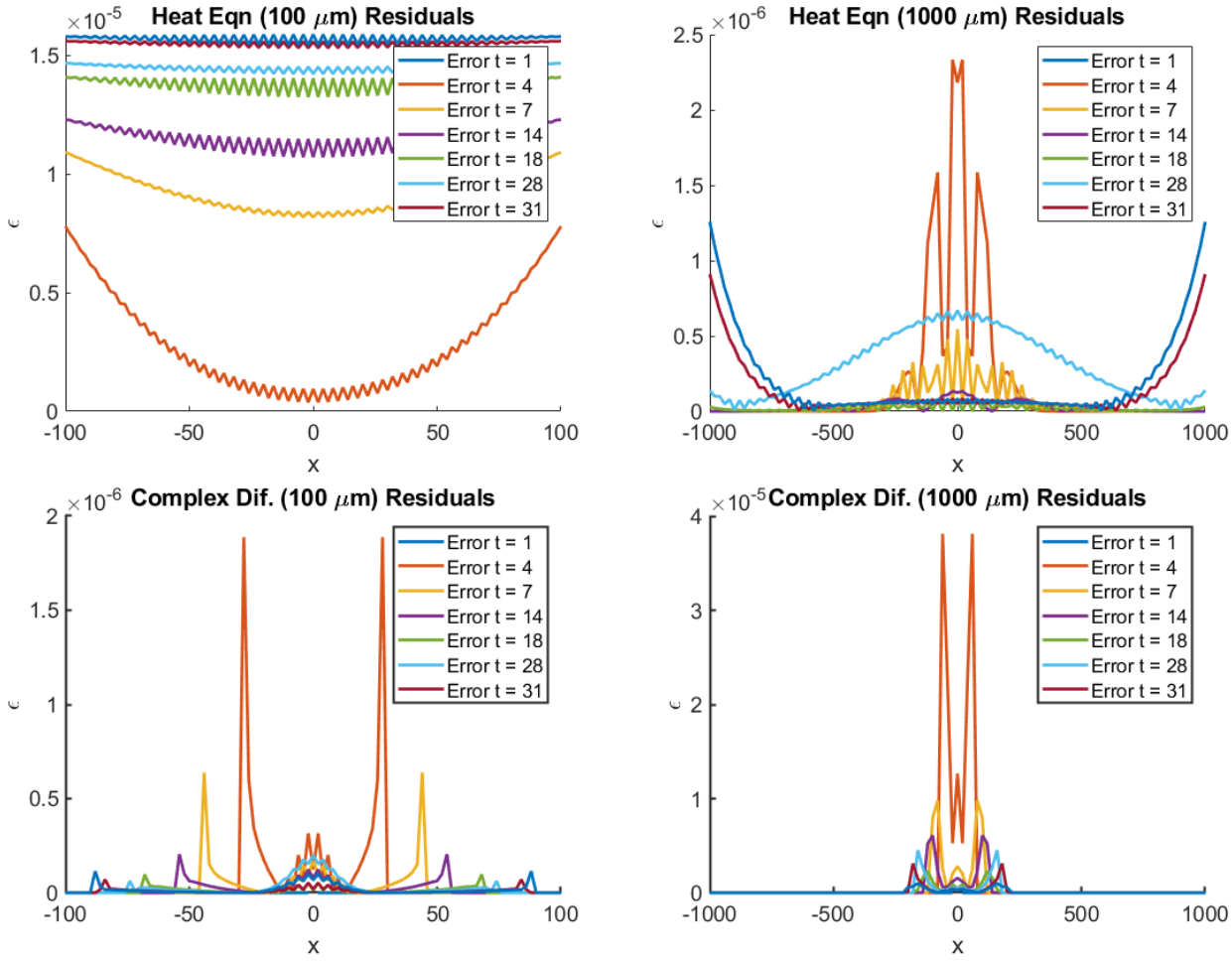

Figure 1: Residual Plots of Diffusion Systems with Varying Domains Lengths Over Time

From the above residual plots it is clear the FDM-solver is accurate to 5-6 significant figures, even under the circumstance of a short domain challenging the validity of solution equation (4).

3.1.2 Travelling Wave Diffusion

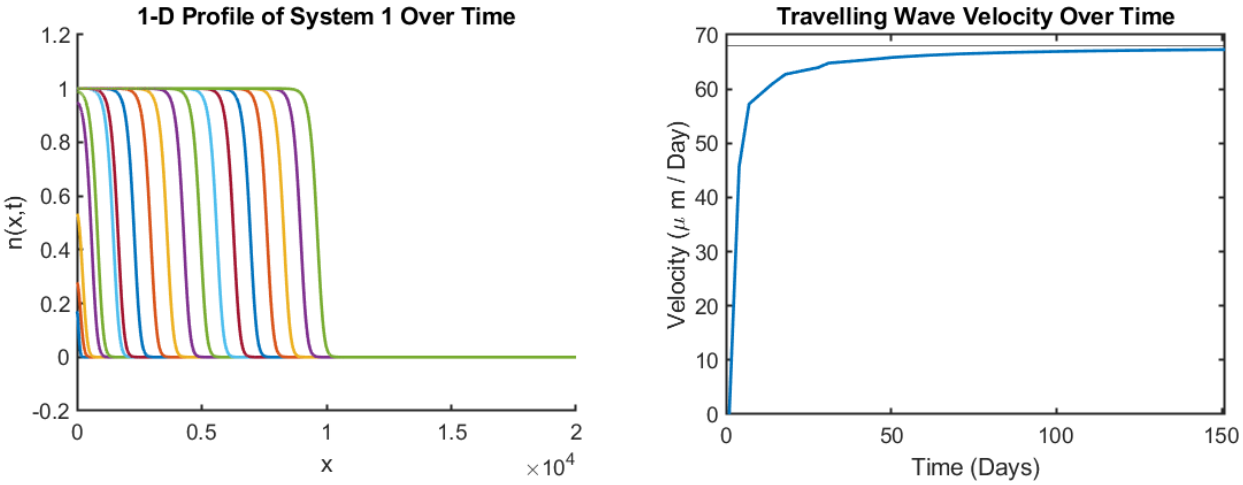

Figure 2: Wave Velocity and Profile Plots Over Time

It is more difficult to verify the overall accuracy of the numerical results generated for this system due to the absence of an analytical solution, however the behaviour of the system over time is as expected from equation (7).

3.1.3 2D *Porous-Fisher* Simulations

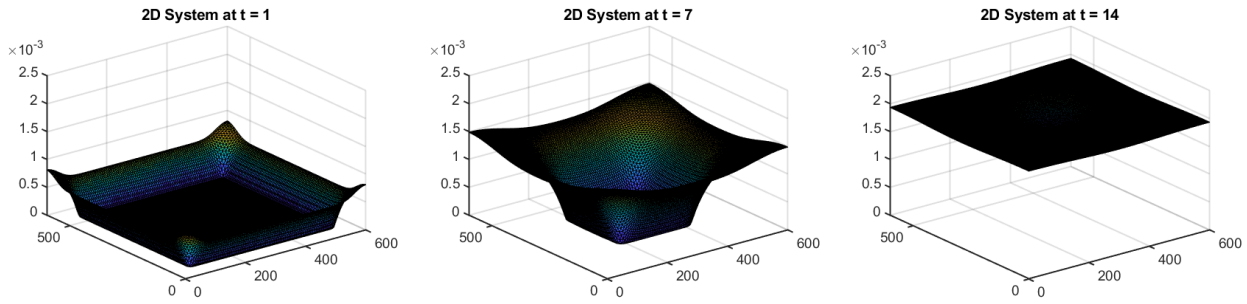

Figure 3: 2D System Profiles Over Time

Using the experimental parameters outlined in Methods, the 2D system bridged after approximately 12.8 days, before stabilising into a steady state. It is important to note that due to physical restrictions, alterations to parameter have little impact on the general behaviour of the system, merely the required time to bridge.

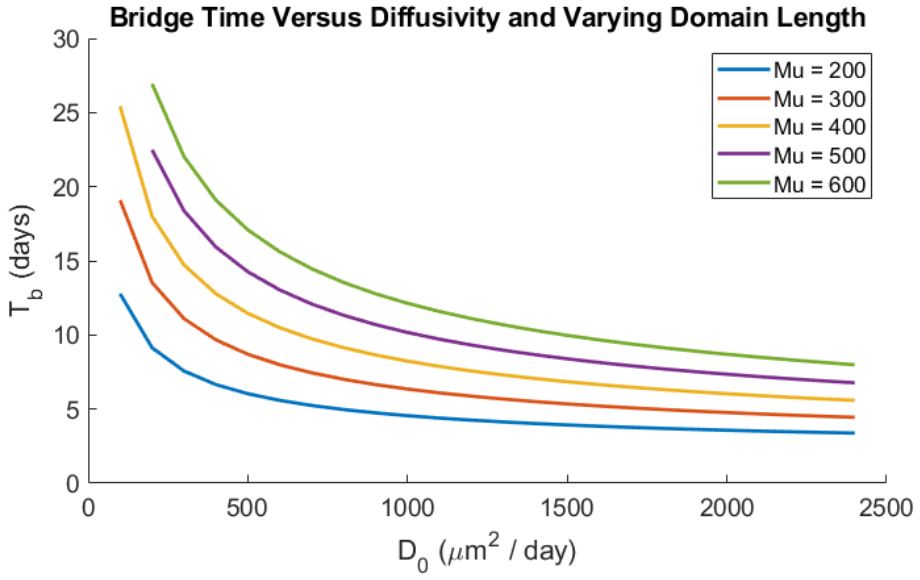

Figure 4: T_b Versus Diffusivity For Varying Domain Lengths

The above figure illustrates the results from the Time to Bridge exercise for a variety of systems, varying across diffusivity and domain length. The results from the plot indicate an exponential relationship between T_b and D (denoted D_0 in Figure 4), regardless of domain length. This is an intuitive result, as increasing diffusivity nonlinearly increases the amount of domain being bridged per unit in time.

3.2 Likelihood Profiling

3.2.1 Quadratic Model

Two separate profiling trials were run with low ($\sigma = 1$) and high ($\sigma = 5$) variance, in order to visualise the impact noise has on the effectiveness of the exercise.

From the Goodness of Fit plots in Figure 5, it can be seen that the high variance trial was dominated by noise, making it more difficult to effectively determine the 'real' behaviour of the observations, compared to the low-variance case where the behaviour is immediately visible. In both variance-cases, the individual parameter profiles are clearly defined, as per the properties of the Gaussian distribution. The 'true' parameter values are indicated with the dashed line, and are contained as likely parameter values in both scenarios. Note that this is not necessarily always the case, due to the random nature of drawing observations, it is possible to draw y^os

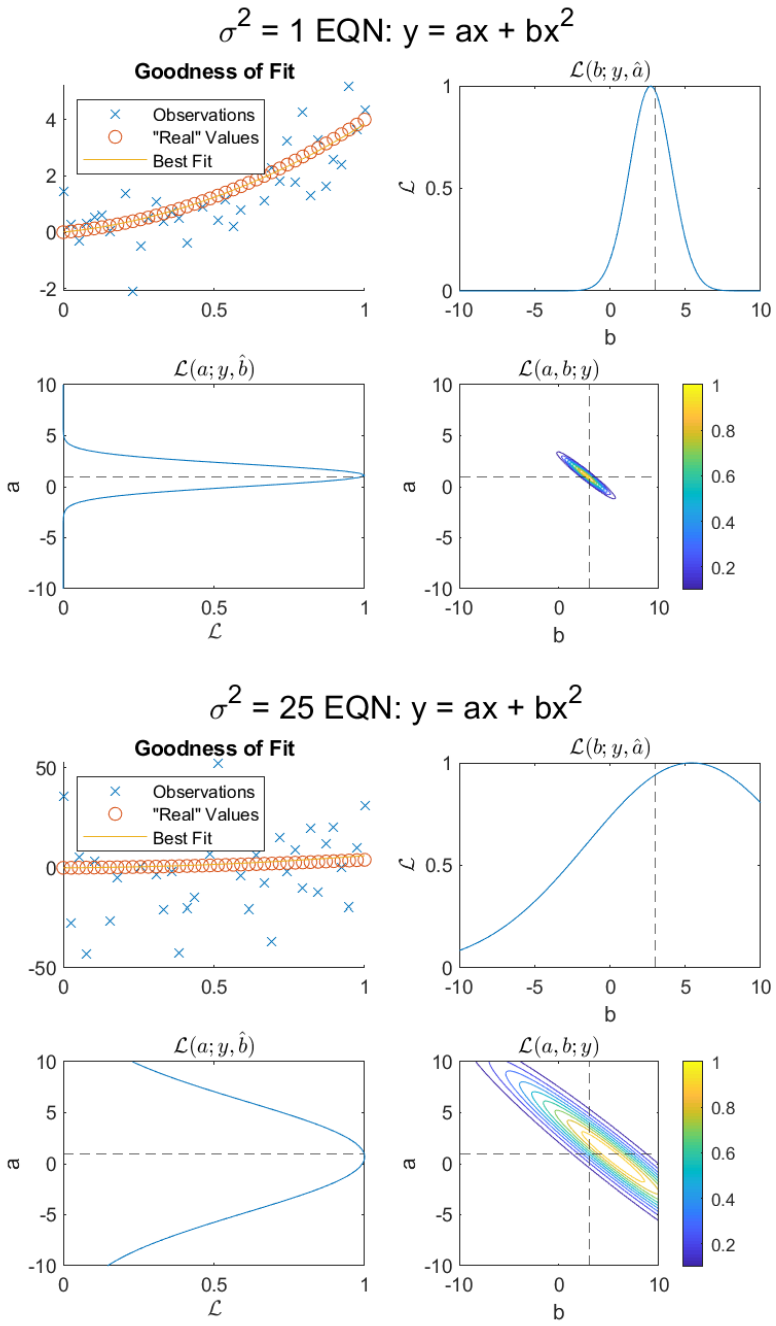

Figure 5: Likelihood Profiles of Quadratic Model Parameters

that infer a more likely set of parameters than the true values.

3.2.2 ODE Model

Like the Quadratic Model, the ODE profiling trials were run with low and high variance cases ($\sigma = 1, 2$ respectively).

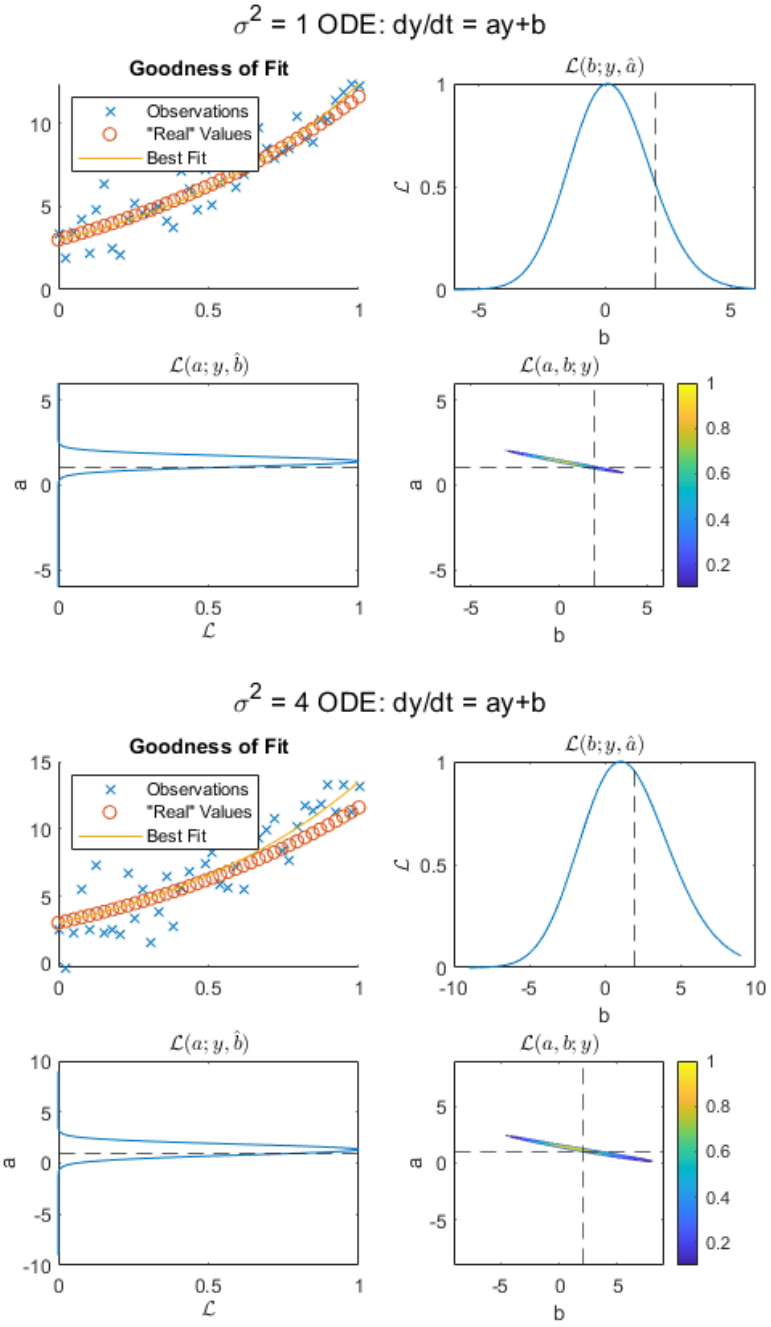

Figure 6: Likelihood Profiles of ODE Model Parameters

Both cases are visibly similar when profiled, and a result of particular note is the greater

variability of the parameter b, compared to a. This is due to the form of the solution to the differential equation, which involves an exponential term, $\exp(at)$. Therefore, alterations to a would produce a far greater change in output than the same change to b.

4 Discussion

4.1 FDM-Solver

With regards to the FDM-Solver's results for the Outward Diffusion scenarios, it is important to note that the simulator achieved 5-6 significant figure accuracy using only first-order forward differencing. First-order differencing was chosen for use with the FDM due to its simplicity, allowing for fast computation of results. This is a significant strength of the FDM-solver's; it combines relatively high accuracy with fast execution.

In many of the residual plots between the initial two systems, there exists visible error 'spikes' that disperse and decrease in severity as system time progresses. One of the partial causes is the resolution of the FDM-solver's mesh used for simulations (101 nodes wide for these cases), resulting in lower accuracy. This particularly pronounces the error in earlier system time, as nearly all of the simulated matter would still be concentrated about $x = 0$. Specifically regarding the complex diffusion system, regardless of time there is evidence of some systematic error, due to the consistent behaviour the spikes across all three trials. For these cases, it is believed to also be caused by the mesh resolution, however it is more visible in the complex diffusion scenario as the analytical solution curves have compact support. This means n values are defined as strictly zero outside of the support area - behaviour which is not enforced in the FDM-solver.

As mentioned previously in Results, the numerical accuracy of solutions for the Travelling Wave scenario cannot be fully verified, except its behaviour can be. Considering the reasonably high level of accuracy shown in the previous scenarios, we assumed that that would be so for this case too. Furthermore, the Travelling Wave exercise was chosen to verify the FDM-solver was correctly displaying the behaviour of a cell-proliferation system, and adhering to constraints such as carrying capacity and the wavespeed bound from equation (7).

Having verified a reasonable level of accuracy for the one-dimensional test cases, we assumed that that would be sufficient to start full 2D simulations of Porous-Fisher. The general behaviour of the system over time was as expected, where the cells proliferated as a travelling wave 'inward' from the outer boundaries into the centre, then ceasing further activity once the system was fully at carrying capacity. It is worth noting that the metric for determining T_b (check if $n(x, y, t) > K/2$), was arbitrarily determined as an appropriate measure, reasoning that there would be sufficient cell density in the area to be considered strongly connected to neighbouring nodes.

For future projects, we aim to further develop the FDM-solver to generate additional, informative outputs beyond 2D simulations and T_b such as 'Gap Radius' - the radius from the system centre to the nearest bridged node - and N, the total number of cells in the system. These outputs can be used *in lieu* of T_b when determining relationships between parameters and could be further developed for different goals in other projects.

4.2 Likelihood Profiling

Profiles for the Quadratic and ODE models were fairly consistent for the selected variances shown in Results, however for some even larger variances (not presented), the level of noise dominating the systems lead to severe numerical instability and invalid results. Some other trials were run with very low variances ($\sigma \leq 0.5$), but were not presented as the lack of meaningful randomness in the observations produced uninformative results. In future work, we aim to apply Likelihood Profiling to the Porous-Fisher FDM-solver itself in order to profile parameters such as D, λ and T_b. Results generated from such a test could identify meaningful bounds on parameters given data drawn from previous experimentation or synthetically generated.

5 Conclusion

The FDM-solver developed for this project can solve the generalised Porous-Fisher equation in one and two dimensions, subject to no-flux boundary conditions, to a reasonably high level of

accuracy with low computational cost. Furthermore, the modularity of the MATLAB code's design allows for the solving of other PDEs, provided the correct parameters are applied to Porous-Fisher, as with the example systems we investigated. By matching the numerical results from the code to the analytical and semi-analytical solutions/behaviours of the example one dimensional systems, we provided evidence that the FDM-solver was correctly accounting for the general behaviour of Porous-Fisher when simulated in 2D. We also performed Likelihood Profiling on two example problems using synthetically generated observations (with 'noise') in order to find probable parameter intervals for their appropriate models. In future research, we aim to incorporate the use of Likelihood Profiling into the FDM-solver, in order to profile parameters such as diffusivity, proliferation rate and time to bridge and investigate the relationship between these values.

References

[1] Murray J, 2002, 'Mathematical Biology: I. An Introduction, Third Edition', *Interdisciplinary Applied Mathematics*, vol. 17, pp. 395-403 & 437-442

[2] Simpson MJ, Jin W, Vittadello ST, Tambyah TA, Ryan JM, Gunasingh G, Haass NK, McCue SW (2018). 'Stochastic models of cell invasion with fluorescent cell cycle indicators.' *Physica A: Statistical Mechanics and its Applications*. 510, 375-386

[3] Simpson MJ, Baker RE, Vittadello ST, Maclaren OJ (2020). 'Practical Parameter Identifiability for spatiotemporal models of cell invasion'. *Journal of the Royal Society Interface*

[4] Jin W, Shah ET, Penington CJ, McCue SW, Chopin LK, Simpson MJ (2016). 'Reproducibility of scratch assays is affected by the initial degree of confluence: experiments, modelling and model selection. *Journal of Theoretical Biology*. 390, 136-145